Dear Reviewer,

Thank you for your nice and constructive comments. We have addressed your comments point-by-point and provided the answer, explanation, and modification where are required in the revised manuscript. This has been uploaded as a supplement file where you can find our answers in a table plus the revised manuscript with track changes.

We hope our answers satisfy your demands.

Best regards,

Jalal Samia and the co-authors

Referees' comments: Author's responses :

Comment	Response
General remarks 1. It should be noted though that this is the fourth publication of the authors with the same dataset for a small study area. I know that such multi-temporal datasets are scarce, but in order to prove the idea I think it is also important to test the concept with other datasets rather than introducing yet another tweak in the methodology.	Thank you for this remark. This is absolutely true, and indeed the concept of landslide path dependency should be explored in other landslides prone areas providing that multi-temporal landslide inventories are available. We have two arguments for this: a) As you mentioned, in order to explore the effect of landslide path dependency, the main requirement is the availability of multi-temporal landslide inventory which to the best of our knowledge (at the starting time of this project, start of PhD of the corresponding author in 2013) was rare. We are now aware of a few more multi-temporal inventories (Asturias in Spain and Ubaye Valley in France), that we are going to use then in a follow-up project if the proposal of that is granted. b) The reason for another tweak in the methodology is that in the implementation of landslide path dependency on landslide susceptibility model in the resolution of slope unit (see Samia et.al, 2018), we found that the performance of landslide susceptibility model did not change substantially. We had this reasoning that the effect of landslide path dependency might be captured better in more finer resolution in the mapping unit of landslide susceptibility model due to the local effect of landslide path dependency. The results of this paper confirmed our previous reasoning. Therefore, this justifies our another tweak in the methodology where we converted the polygons of landslides to point, and then used a new metric (Ripley function) to quantify the effect of landslide path dependency. Having said, and considering the substantial importance of landslide path dependency on the performance of landslide susceptibility model, we believe that landslide path dependency is an important component in landslide susceptibility definition, and this should be further explored in other landslide prone areas.
General remarks 2. It is also hard for me to follow the interpretation and conclusion that the models considering path dependency are "substantially" better than the conventional one. With the information provided I consider it hard to take a decision at all, but I would tend to rate the conventional model as the best, see also my comments below.	The conclusion comes from the comparison of performance of three landslide susceptibility models with the metrics of AUC and AIC. This improvement comes from adding only two variables reflecting landslide path dependency to the existing 16 DEM-derivatives. An increase from the AUC of conventional susceptibility model with the value of 0.704 to the AUC value of 0.764 for the conventional plus path dependent susceptibility refers to "substantial" improvement of landslide susceptibility model. Also, AIC values for conventional plus path dependent and purely path dependent landslide susceptibility models are lower

	(11711 and 12469) which are lower than the AIC value of conventional susceptibility model (12678).
General remarks 3. I think it is necessary to also show the detailed susceptibility maps of the conventional model to be able to compare the spatial performance. In all path dependent susceptibility maps it is obvious that the path dependent variables clearly dominate the spatial distribution of landslide susceptibility (bullseye artifacts). Are those "hot spot" susceptibility maps useful in practice? Are the models well-balanced?	Regarding the detailed maps of conventional susceptibility see our answers in the comment number 14 in the below. we have considered your comment regarding the applicability of dynamic landslide susceptibility maps in practice as following: "In reality, static susceptibility maps created (either with a conventional susceptibility model, or as the static portion of a conventional plus path dependent model) can be used in sustainable planning whereas dynamic susceptibility maps can be considered in short-term land use planning." The hotspots in the susceptibility maps of conventional plus path dependent and purely path dependent landslide susceptibility, show the predicted susceptibility per time slice given the history effect of previous landslides. Surely those hotspots are useful in practice in that given period as it reflects that newly happened landslides have higher susceptibility level demonstrating more cares for practical purposes. We are not quite sure what you mean with well-balanced model but our datasets used in the three susceptibility models are balanced.
General remarks 4. The conventional model probably has a poor variability as it only contains DEM derived variables. What happens if more fundamental information is introduced, like lithology? I understand that it was intended to use a model with minimal data requirements, but it also hast to be demonstrated first that this works comparing it to a more complex dataset.	Thank you for this point. Aa you also have mentioned, this was our aim to model landslide susceptibility using minimum data requirements (DEM-derivatives) plus variables derived from landslide path dependency. However, we did that work and it's just not in the paper. The conventional susceptibility modelled by DEM-derivatives, geology and land use has lower model performance (AUC = 0.771) when adding two landslide path dependency variables in the conventional plus path dependent landslide susceptibility (AUC = 0.801). Considering your comment, we also feel that this could be mentioned in the discussion of paper as following: "More complex explanatory variables such as geology, soil and land use can also be used along with DEM-derivatives to improve landslide susceptibility models and maps. However, these are not always available. In fact, considering landslide path dependency effect into such complete explanatory factors improve their performance as well. We confirmed this in an additional

	exploration where we constructed a conventional landslide susceptibility model used in this paper, with the same DEM-derivatives, but also with land use and geology as explanatory factors. The results demonstrated that adding our two landslide path dependency variables to such an improved conventional landslide susceptibility increased its performance (from AUC value of 0.771 to AUC value of 0.801)."
General remarks 5. The methodology is also not completely clear to me based on the explanations provided. Were models produced for different time slices or only one model for each parameter set?	Indeed the methodology for modelling part is not completely clear. We have updated the manuscript in this matter (in line 216-220) as following: "Conventional landslide susceptibility was modelled using DEM-derivatives only once for the defined training dataset and was tested using the independent testing dataset. Conventional plus path dependent landslide susceptibility model was constructed using DEM-derivatives plus the two landslide path dependency variables. The purely path dependent landslide susceptibility was modelled only by using the two landslide path dependency variables. All three models were constructed only once."
Methodology 6. E.g. L 94-98: To better understand the whole concept it would be good to understand how the authors define "follow-up landslides" and if/how they are for example discriminated from reactivated landslides.	This comment is confusing since in the lines of 94-98, we did not talk about follow-up landslides at all. However to make it clear, in our previous paper in Samia et al, 2017, we introduced for the first time the term "follow-up landslides" and differentiated that from reactivated landslides as following: "Note that follow-up landslides are not reactivated landslides. We consider a landslide a reactivated landslide when all or most of the landslide moved down again, under the same general condition as the first landslide. Instead, follow-up landslides are new landslides that have different size and shape than the pre-existing landslide." In the current manuscript when talking about follow-up landslides (mainly in the discussion), the proper reference has been provided.
Methodology 7. L 112-113, Fig. 1: Is this figure not taken from Samia et al. 2017a or b?	Yes, it is taken from those papers , and also from our paper in Samia et al, 2018. We have added those two references in the updated manuscript.

Methodology 8. L 183, Fig. 5: The figure is not referred to in the text. Is it correct that the arrows on the left point from the start to the results? Are they not supposed to start at the Smoothed STC sketch?	Thank you for this point, indeed the figure is not referred in the text. Now we have provided reference for this figure in the line of 175 where we talk about the computation of the two landslide path dependency variables. Also we appreciate your comment about the position of arrows in Fig. 5. You are right and we corrected the figure in the updated manuscript.
Methodology 9. L 205-215: I am not sure if I understand the composition of the training and testing data and the whole procedure. Were the models trained on a single time slice from L 201 each and then tested with the subsequent testing time slice from L 202? Then 10 samples were taken for each time slice? How were the results in tables 1 and 3 generated from the different time slice models? Maybe the methods section could be put more clearly.	No, the model was trained to the combination of time slices 1947, 1954, 1981, 1985, 1999, May 2004, March and May 2010. After that, the model was tested on testing dataset which is the combination of time slices of 1965, 1977, 1991, 1997, December 2004 and 2005 and April 2013 and 2014. Then, due to the unequal amount of pixels with and without landslide in each of these training and testing datasets, we selected 5000 pixels with landslides and 5000 pixels without landslides randomly in each of training and testing dataset. This random selection was repeated 10 times in both training and testing datasets. Therefore, for each of these 10 random datasets, conventional, conventional plus path dependent and purely path dependent landslide susceptibility models were constructed, and the results presented in the table 1 and table 3, are the average of these 10 models. To make this part more clear, we have modified sentences in the lines of 200-203 as following: "To achieve this, all landslides in the time slices of 1947, 1954, 1981, 1985, 1999, May 2004, March and May 2010 were used for training, and all landslides in the time slices of 1965, 1977, 1991, 1997, December 2004 and 2005 and April 2013 and 2014 were used for testing (Figure 1)." Also sentences in the lines of 209-213 were updated as: "Therefore, we randomly selected 5,000 pixels with landslides and 5,000 pixels without landslides from both training and testing datasets in order to create equal datasets both for training and testing of the models. This random selection of pixels was repeated 10 times both in the training and testing datasets. Therefore, we trained the conventional, conventional plus path dependent and purely path dependent landslide susceptibility 10 times, and finally tested 10 times as well."

Results and discussion 10. L 218-219: Is it possible to show a map of what the variables reflecting the path dependency look like spatially?	No that's not possible. We can only make prediction from these variables depending when and where previous landslides happened. We have already shown the examples of the predictions from landslide path dependency variables in our existing figures 8 and 9.
Results and discussion 11. L 225, Fig. 6: What does the color code represent?	The colors represent the intensity of STC measure. We have added two sentences to the caption of figure 6 to make this clear as following: "The colours represent the intensity of STC measure. Red colour indicates high STC and green indicates low STC."
Results and discussion 12. L 228-230: Isn't a spatial scale of 60 m quite small? Because 60 m can be below the size of a single landslide. Are these new landslides or reactivated ones?	We noted that the 60 meters is the characteristic spatial scale of the exponential function so that substantial effects still exist over distances more than hundred meters. Moreover, this has been calculated from centre point to the centre point of different landslides and so if the centre points are 60 or 100 or 150 meters away from each other, they could still be not overlapping or overlapping and they could be either new or reactivating landslide. This empirical procedure does not distinguish between new and reactivated landslides.
Results and discussion 13. Table 1, Table 3: Are the results available for different time slices? It is unclear to me which results are presented here. Is this a summary of all time slice models? Or the best models?	Considering the explanations given above in the methodology part, the results presented in these two tables should already be clear. However, to make this even more clear, we have modified the caption of table 1 and table 3 as following: "The values of AUC represent the average AUC values in the 10 training and 10 testing datasets. The values of AIC represent the average AIC values in the 10 training datasets." "Contingency tables computed with cut off value of 0.5 for the three models. The numbers in the table represent the average values computed in the 10 training and 10 testing datasets."
Results and discussion	We have explained this in above. Just to recall, this conclusion comes from the comparison of AUC and AIC values of these three models and not based on the

14. Section 5.2, Table 3: I do not agree with the interpretation that the conventional plus path dependent and path dependent models are substantially better than the conventional one. The conventional one has slightly more hits and less misses (false negative). In my opinion, false negatives are more critical than false positives, which actually contribute to a better zonation when the goal is not the accurate detection of landslides but the identification of susceptible areas. It would be interesting to see also the susceptibility maps (like figures 8 and 9) for the conventional models to be able to better compare their spatial performance. Success rate curves plotting the distribution of landslides over the susceptibility classes would add more information.	values presented in table 3, which result only from an arbitrary 0.5 cut off value. It's not possible to make conventional susceptibility map like the dynamic path dependent susceptibility maps in figure 8 and 9 because only one conventional landslide susceptibility map was made based on the conventional definition of landslide susceptibility which is a time-invariant concept. The relevant spatial comparison is shown in figure 7 where we show the static susceptibility map from conventional model along with examples from one time slice of the other two path dependent dynamic models. We have provided the success rate curves for three models in 10 training datasets and also for the testing datasets as new figure 7 in the revised manuscript.
Results and discussion 15. L 235-237 and L 339-341, using only path dependent variables: I do not understand, why should we want to predict landslides just based on past landslides? Firstly, at this point multi-temporal landslide inventories are rarely available and secondly, this is in my opinion in disagreement with the fundamental paradigm of data-driven landslide susceptibility analysis, which is deducing landslide occurrence from independent variables. Also, the susceptibility maps based on the path dependent variables only have extreme bullseye effect artifacts and I doubt that the maps are in this form useful for practical implementations.	Thank you for this interesting question and comment. Well, we – for the first time – have challenged the conventional definition of landslide susceptibility with introducing the new concept of path dependency indicating the history effect of landslides on future susceptibility (Samia et al, 2017). With this, landslide susceptibility is not a function that considers only the spatial distribution of landslides along with a set of independent environmental factors but path dependency also needs to be taken into account. This effect was found in exploration of a unique and rich multi-temporal landslide inventory in Collazzone, Italy. Landslide path dependency in this study area indicated that susceptibility is not time-invariant but susceptibility changes over time. With this, a new paradigm for landslide susceptibility is emerging called dynamic path dependent susceptibility which requires exploration of the existence of path dependency, characterization and quantification of such effect, and finally its implementation in landslide susceptibility modelling. This modifies the fundamental paradigm of susceptibility in two aspects: first, spatial and temporal effect of landslide path dependency is an "add-on" dependent variable that has to be considered in combination with independent environmental factors. Second, landslide susceptibility is not time-invariant but instead is dynamic and changes over time. In our study area, this effect was obvious, and had a strong effect on the performance of landslide susceptibility models. However, this new paradigm is in its initial stage and has to be explored and studied in other landslide prone

	areas where detailed multi-temporal landslide inventories are available. We are aware that such multi-temporal inventories are rare but given the substantial progresses made already in remote sensing imagery and techniques, and in near future, this will provide room for creation of more multi-temporal landslide inventories where we believe would be main future direction in the field of landslide mapping and documenting.
Results and discussion 16. Figures 7, 8 and 9: - the maps would be easier to interpret with a hillshade in the background and the outlines of the corresponding training and/or test landslides, which are required to assess the spatial performance of the models.	Thank you for this point. We have added the hillshade to the backgrounds of landslide susceptibility maps in the revised manuscript. However, it would not be helpful to show the outlines of landslide because there are too many landslides and they completely cover the area.
- it is a good idea to show the distribution of the susceptibility classes, but pie charts are not very effective for comparing multiple part-to-whole relationships. They are inconvenient to read and it is hard to perceive the quantitative relationships. Bar or column charts would be more suitable.	We appreciate the different preference but we feel that pie charts work better for this study.
- why are there blank/white areas in the maps containing path dependent variables?	The reason is that the model does not make a prediction for those areas because one of the explanatory factors contains no data in those areas. This factor is topographic position index (TPI) and it has no data in those areas because the slope is zero. The issue only occurs in the conventional plus path dependent model because only that model uses TPI as explanatory factor. It is easy to assign values of zero to TPI in those areas and then calculate the model with that manually changed TPI but we felt that would not be fair. By using TPI and the conventional plus path dependent model with no data we are underestimating model performance because no landslides occurred in any of no data areas and predictions would be zero if we assign zero values to TPI.
Results and discussion 17. L 345: I think this should be the map on the left in Figure 7.	Thank you for your sharp observation. This has been corrected in the updated manuscript.
Results and discussion 18. L 347-349, usage of landslide susceptibility maps for amount of time of landslide inventory: I think this is hard to generalize and depends on the task, but for sustainable planning of resilient urban areas I would rather counsel time-insensitive susceptibility models based on intrinsic parameters.	We certainly agree with you. The usage of landslide susceptibility maps indeed depends on the goal and task of audience. We also fully agree with you that for sustainable planning the conventional static landslide susceptibility maps are more useful. However, we believe that the dynamic path dependent landslide susceptibility maps would be also useful both in long-term and short-term planning. The dynamic path

	dependent landslide susceptibility maps consist of a static part taking intrinsic factors into account, and a dynamic part taking landslide path dependency into account. As you also have mentioned, the susceptibility maps in the static part are optimal for sustainable planning. However, if it's possible to compute the full dynamic susceptibility maps as in the Collozzone area, then this would be even more practical both for short-term and long-term planning. Another important point is that the only dynamic part of path dependent landslide susceptibility maps would be also in the interest of short-term land use planners and farmers where they would be aware of the areas with different intensity of landslide susceptibility. As we discussed above, we have updated that part of manuscript in the revised version as following: "The usage of conventional static landslide susceptibility maps and dynamic landslide susceptibility maps taking landslide path dependency depends on the goal and task of audience. In reality, static susceptibility maps created (either with a conventional susceptibility model, or as the static portion of a conventional plus path dependent model) can be used in sustainable planning whereas dynamic susceptibility maps can be considered in short-term land use planning."
19. Figure 10: I do not understand what hypothetical means. Is this graph based on real data or is this just a sketch?	This is just a hypothetical sketch. We have updated this in the revised manuscript as following: "Conceptual model of implication of dynamic path dependent landslide susceptibility model in landslide hazard assessment."

1   **Dynamic path dependent landslide susceptibility modelling**

2   Jalal Samia [1, 2], Arnaud Temme [3, 4], Arnold Bregt [1], Jakob Wallinga [2], Fausto Guzzetti [5], Francesca Ardizzone [5]

3   [1] Laboratory of Geo-Information Science and Remote Sensing, Wageningen University & Research, 6708 PB
4   Wageningen, Droevendaalsesteeg 3, The Netherlands

5   [2] Soil Geography and Landscape group, Wageningen University & Research, 6708 PB, Wageningen,
6   Droevendaalsesteeg 3, The Netherlands

7   [3] Department of Geography, Kansas State University, 920 N17th Street, Manhattan, KS, 66506, United States

8   [4] Institute of Arctic and Alpine Research, University of Colorado, Campus Box 450, Boulder, CO 803309-0450,
9   Colorado, United States

10   [5] Istituto di Ricerca per la Protezione Idrogeologica, Consiglio Nazionale delle Ricerche, via Madonna Alta 126,
11   06128 Perugia, Italy

12   **Correspondence**: Jalal Samia, jalal.samia@wur.nl, +31617699436, +31 (0)317 – 419000

13

14   **Abstract**

15   This contribution tests the added value of including landslide path dependency in statistically-based landslide
16   susceptibility modelling. A conventional pixel-based landslide susceptibility model was compared with a model
17   that includes landslide path dependency, and with a purely path dependent landslide susceptibility model. To
18   quantify path dependency among landslides, we used a Space-Time Clustering (STC) measure derived from
19   Ripley's space-time K function implemented on a point-based multi-temporal landslide inventory from the
20   Collazzone study area in central Italy. We found that the values of STC obey an exponential decay curve with
21   characteristic time scale of 17 years, and characteristic space scale of 60 meters. This exponential space-time decay
22   of the effect of a previous landslide on landslide susceptibility was used as the landslide path dependency
23   component of susceptibility models. We found that the performance of the conventional landslide susceptibility
24   model improved considerably when adding the effect of landslide path dependency. In fact, even the purely path
25   dependent landslide susceptibility model turned out to perform better than the conventional landslide susceptibility
26   model. The conventional plus path dependent and path dependent landslide susceptibility model and their resulted
27   maps are dynamic and change over time unlike conventional landslide susceptibility maps.

28

29   **1. Introduction**

30   Landslide susceptibility modelling calculates the likelihood of landslide occurrence in a certain location (Brabb,
31   1985). The resulting landslide susceptibility maps from landslide susceptibility models indicate where landslides
32   are likely to occur (Guzzetti et al., 2005). These maps are useful in land use planning and insurance, among others.
33   In this context, different methods and techniques have been used for landslide susceptibility modelling.

Reichenbach et al. (2018) classified these methods and techniques into five groups: (i) direct geomorphological mapping, (ii) analysis of landslide inventories, (iii) heuristic or index-based approaches, (iv) physically or process-based methods, and (v) statistically-based techniques.

Statistically-based landslide susceptibility techniques have been the preferred technique in the modelling of landslide susceptibility (Reichenbach et al., 2018). In statistical landslide susceptibility modelling, empirical quantitative relations are explored between the spatial distribution of landslides and a set of environmental factors (e.g., slope and geology) (Van Westen et al., 2003; Guzzetti et al., 2005). The spatial distribution of historic landslides, documented in landslides inventories, is therefore a crucial input for statistically-based landslide susceptibility modelling (Guzzetti et al., 2012; Van Westen et al., 2008). Direct field mapping, visual interpretation of aerial photographs and other remote sensing images are the main sources for such mapping of landslide inventories (Guzzetti et al., 2012). Landslides in such inventories are stored as points or polygons. Although polygon-based landslide inventories (Ardizzone et al., 2018; Schlögel et al., 2011; Galli et al., 2008) are becoming increasingly available, in many landslide prone regions only less-detailed point-based landslide inventories are collected (Gorum et al., 2011; Sato et al., 2007; Keefer, 2000). Conditioning attributes used in landslide susceptibility modelling are mainly derivatives of digital elevation models (DEMs) along with geological, soil and land use data (Günther et al., 2014; Neuhäuser et al., 2012; Reichenbach et al., 2018). While geology, land use and soil data are not always available in high detail, DEM-derivatives are easily computed and globally available at a range of resolutions. Therefore, the minimum available dataset for landslide susceptibility modelling includes a point-based landslide inventory and a set of DEM-derived conditioning attributes.

Traditionally, landslide susceptibility is considered time-invariant: susceptibility of a place to landslide occurrence is constant over time, at least over decadal scales. Recently, we proposed the concept of time-variant landslide susceptibility, where susceptibility changes over time due to the transient effect of previous landslides on future landslide occurrence (Samia et al., 2017b, a). We referred to such a transient effect as "path dependency", a term adopted from complex system theory where it is used to describe the concept that the history of a system specifies the future behaviour of a system through legacy effects (Phillips, 2006). In our study area in Umbria, central Italy (Figure 1), we identified the existence of path dependency among landslides: earlier landslides locally increased the susceptibility for future landslides for about two decades, during which the susceptibility decays exponentially over time (Samia et al., 2017b). We first implemented the effect of this landslide path dependency in landslide susceptibility modelling at the scale of slope units. Such units divide an area into hydrological units bounded by drainage and divide lines (Carrara et al., 1991; Alvioli et al., 2016). We found that the impact of path dependency on landslide susceptibility models at slope-unit scale was limited (Samia et al., 2018). This limited impact of landslide path dependency on model predictions was probably due to the fact that landslide path dependency affects landslide patterns at spatial scales smaller than slope units, and we hypothesized that differences between models were likely to increase when including path dependency at smaller spatial scales.

The objective of this work is thus to consider the effect of landslide path dependency in landslide susceptibility modelling at the resolution of 10×10 m pixels. We hypothesize that including landslide path dependency will improve the performance of landslide susceptibility models. We also explore whether a purely path dependent landslide susceptibility model, i.e. based solely on landslide inventory information, can provide a meaningful

2

72   landslide susceptibility map. We use the unique multi-temporal landslide inventory from the Collazzone study area

73   (Figure 1) (Guzzetti et al., 2006a; Ardizzone et al., 2007; Ardizzone et al., 2013).
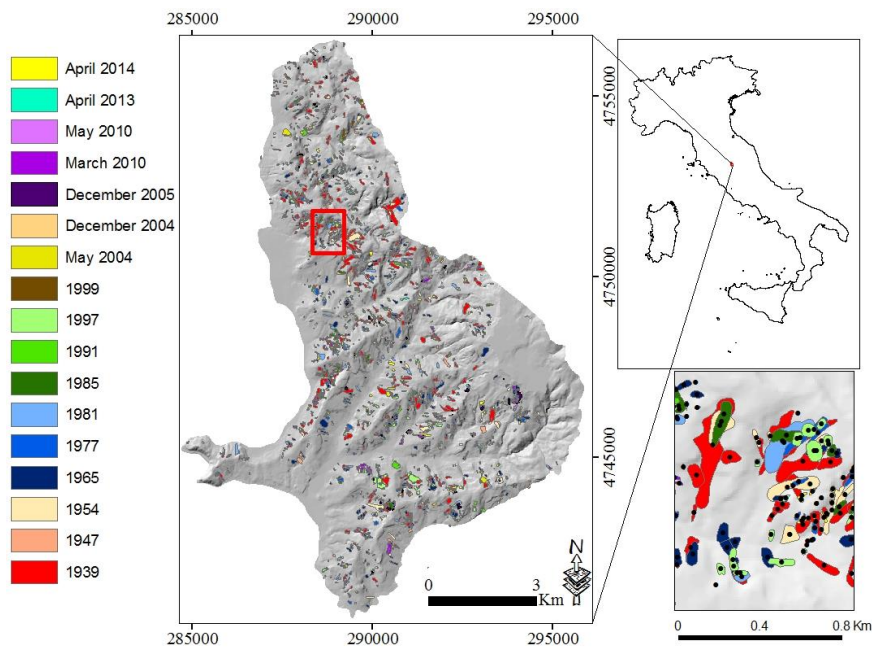
2. Study area and data

75   The Collazzone study area, Umbria, central Italy (Figure 1), extends for about 80 km^2 with terrain elevation

76   between 140 to 632 m and terrain slope derived from a 10×10 m DEM (Figure 2) between 0 to 64°. The DEM

77   was prepared by interpolating 5- and 10-m contour lines shown in 1:10,000 topographic maps (Guzzetti et al.,

78   2006b). A set of DEM-derivatives that has been widely used in landslide susceptibility modelling was computed

79   in SAGA GIS and ArcGIS. We expect that these DEM-derivatives capture topographical, geomorphological and

80   hydrological properties of locations in our study area.

81   The DEM-derivatives (Figure 2) are slope angle, curvature, plan and profile curvature, aspect, northness and

82   eastness as cosine and sine transformations of aspect, topographic position index (TPI) representing different

83   geomorphological settings (Costanzo et al., 2012), stream power index (SPI) representing the erosive power of

84   streams (Moore et al., 1993), topographic wetness index (TWI) as an index for hydrological process in the slope

85   (Jebur et al., 2014). Additionally, for every pixel we computed the distance to the nearest river, the slope length

86   and steepness factor (LS factor) as an index for soil erosion on slope (Moore and Wilson, 1992), the vertical

87   distance to the slope's channel network, and relative slope position representing the relative position of slope in

88   cells between the valley bottom and ridgetop. Additionally, we calculated topographic roughness, which expresses

89   the difference in the values of elevation in the neighbouring cells in the DEM (Riley et al., 1999), and the standard

90   deviation of elevation and slope in a 3×3 pixel window. These 16 DEM-derivatives were used as independent

91   explanatory variables in logistic regression for modelling of landslide susceptibility (see section 3.2).

92   Landslides are abundant in this area, and range from recent shallow landslides to old deep-seated landslides

93   (Guzzetti et al., 2006a). Intense and prolonged rainfall and rapid snowmelt are the main triggers of landslides in

94   the area (Cardinali et al., 2000; Ardizzone et al., 2007). A unique multi-temporal landslide inventory with 3391

95   landslides has been mapped in 19 different time slices. The age of the landslides ranges from relict and very old

96   landslides with an uncertain date of occurrence to landslides that have occurred in 2014. Aerial photographs, direct

97   geomorphological field mapping and satellite images were used for the preparation of the multi-temporal landslide

98   inventory (Ardizzone et al., 2013; Guzzetti et al., 2006a; Galli et al., 2008). Only time slices of the multi-temporal

99   inventory for which the relative date of occurrence is known (Figure 1), were used in this study because time

100 between landslides is a key element in the quantification of landslide path dependency (Samia et al., 2017a, b). In

101 addition, the first time slice, with the known date of 1939, was only used in the computation of the landslide path

102 dependency parameters, and not in landslide susceptibility modelling because of its unknown past. Ultimately, a

103 multi-temporal landslide inventory was used that contains distribution of landslides in 16 time slices dating from

104 1947 to 2014 (Figure 1). This multi-temporal landslide inventory was mostly prepared at the scale of 1:10,000

105 which is sufficient for conversion to a 10×10 m pixel-based landslide inventory. However, time slices from 1939

106 to 1997 were prepared from aerial photographs with scales ranging from 1:15,000 to 1:33,000, and this may

107 introduce some positional inaccuracy in landslides, in the order of one pixel. Given that the median size of landslide

108 in this period is 19 pixels, we believe that this is an acceptable level of inaccuracy.

3

109 More information about the Collazzone study area and the multi-temporal landslide inventory is given in (Galli et
110 al., 2008; Guzzetti et al., 2006a; Guzzetti et al., 2009; Ardizzone et al., 2007).

111

112 **Figure 1.** Multi-temporal landslide inventory dating from 1939 to 2014 (left map) (adapted from (Samia et al.,
113 2018; Samia et al., 2017a, b)). Collazzone study area and Umbria region (right upper map). The coordinate system
114 of maps is EPSG:32633 (www.spatialreference.org). Landslide points were constructed by placing a point in the
115 geometric centre of each landslide polygon (map in the right lower corner). The red rectangle shows the extent of
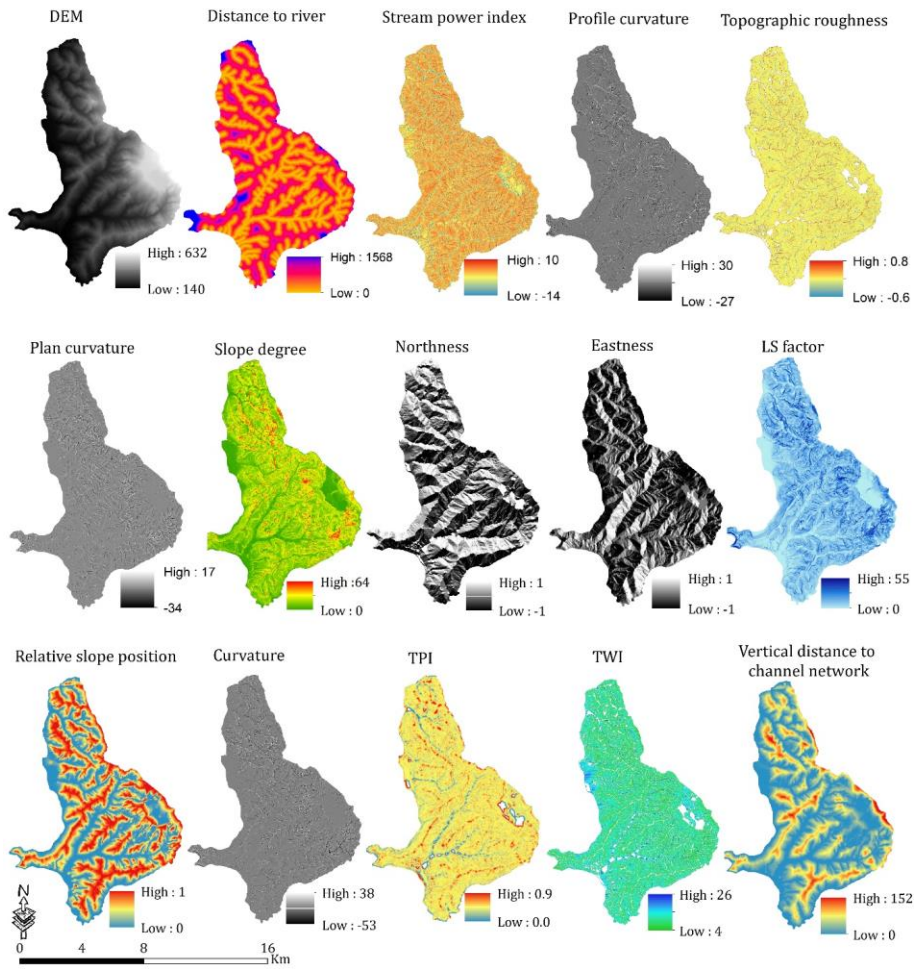116 the map in the lower right.

4

Figure 2. DEM (digital elevation model) and its derivatives used in conventional and conventional plus path dependent landslide susceptibility models. TPI means topographic position index, TWI means topographic wetness index and LS factor stands for slope length and steepness factor.

3. Methods

We used logistic regression to construct three different landslide susceptibility models (Figure 3): (i) a conventional landslide susceptibility model using DEM-derivatives, (ii) a conventional plus path dependent landslide susceptibility model using 16 DEM-derivatives and two landslide path dependency variables (explained below), and (iii) a purely path dependent landslide susceptibility model using only the two landslide path dependency variables. We compared the performance of these models using Area Under Curve (AUC) values from the Receiver Operating Characteristic (ROC) (Mason and Graham, 2002), and selected the optimal model using

128 the Akaike Information Criterion (AIC) (Akaike, 1998), which penalizes the use of additional variables in a model.
129 Ultimately, the coefficients of the variables selected by three landslide susceptibility models and the resulting
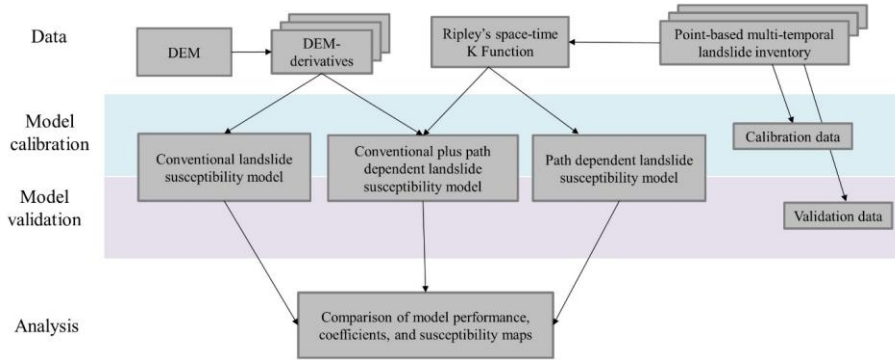130 landslide susceptibility maps were compared.

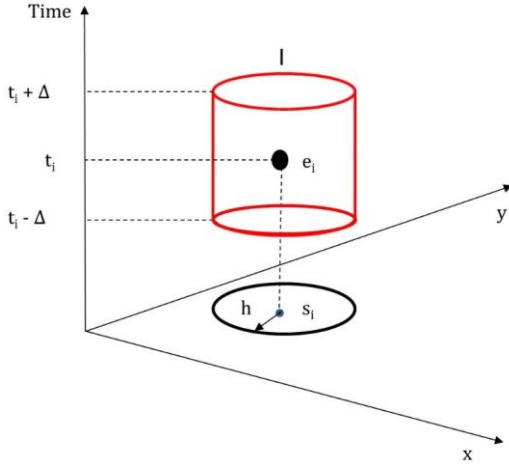131 **Figure 3.** Flowchart of methods

132

133 **3.1 Quantifying landslide path dependency using Ripley's space-time K function**

134 The spatial-temporal dynamics of landslide path dependency was recently quantified for the Collazzone study area
135 (Samia et al., 2017a), and was implemented in landslide susceptibility modelling at the scale of slope units (Samia
136 et al., 2018). Our previous quantification of landslide path dependency used simplified information about the
137 spatial overlap among landslides in a polygon-based multi-temporal landslide inventory (Samia et al., 2017b). The
138 novel aspect of the present paper is that now, at finer spatial resolution, we quantify landslide path dependency
139 simultaneously in space and time. For this quantification, we use Ripley's K function (Ripley, 1976; Diggle et al.,
140 1995). Ripley's K function has been used mainly in spatial point pattern analysis and reflects the degree of spatial
141 clustering of events (e.g., landslides (Tonini et al., 2014), forest fire (Gavin et al., 2006), crimes (Levine, 2006)
142 and disease outbreaks (Hinman et al., 2006)). The function determines whether events are clustered, dispersed or
143 randomly distributed. A modified Ripley's K function was also used to quantify the degree of clustering of point
144 events in space and time (Lynch and Moorcroft, 2008; Ye et al., 2015). In the landslide path dependency context,
145 we used Ripley's space-time K function to reflect the degree to which landslides occur near previous landslides,
146 and how this changes with increasing distance to the previous landslide in space and time. The starting point to
147 derive Ripley's K is a point-based multi-temporal landslide inventory consisting of points in the geometric centre
148 of polygons of landslides (Figure 1).

149 Ripley's space-time K function tests whether the number of events that is observed in a space-time cylinder around
150 an initial event is equal to what is expected given the average point density in space and time (Ripley, 1976, 1977;
151 Diggle et al., 1995). The space-time cylinder $I_{(h, \Delta)}$ (Figure 4) is defined as:

152 $$I_{(h,\Delta)} \left(d_{ij}, t_{ij} \right) = \begin{cases} 1, \left(d_{ij} \leq h \text{ and } \left(t_{ij} \leq \Delta \right) \right) \\ 0, otherwise \end{cases} \quad (1)$$

6

153 where h shows the spatial distance increment, Δ shows the time increment, i and j are two landslide centre points,
154 and d and t reflect the distance and time between the two landslide centre points, respectively.

155 **Figure 4.** Space-time cylinder neighbourhood (Smith, 2016) for a landslide event (e_i)

156 The expected Ripley's K function for one space-time cylinder of size h and Δ is defined as:

157 $$K(h,\Delta) = \frac{1}{\lambda_{st}}\sum_{j \neq i} E\big[I_{(h,\Delta)}\,(d_{ij}, t_{ij})\big] \qquad (2)$$

158 where E is the expected number of landslides in the cylinder, and λ_{st} reflects the average space-time intensity of
159 the landslides i.e., the expected number of landslides per unit of space-time volume, which is calculated as:

160 $$\lambda_{st} = \frac{n}{a(R)\times(t_{max}-t_{min})} \qquad (3)$$

161 where n is the number of landslides in the entire inventory, t is time, and $a(R)$ reflects the size of the area. Therefore,
162 the expected Ripley's space-time K function for the space-time cylinders around each landslide point is defined
163 as:

164 $$K(h,\Delta) = \frac{1}{n.\lambda_{st}}\sum_{i=1}^{n}\sum_{j \neq i} E\big[I_{(h,\Delta)}\,(d_{ij}, t_{ij})\big] \qquad (4)$$

165 Similarly, the observed Ripley's space-time K function is calculated from the landslide inventory as:

166 $$\hat{K}(h,\Delta) = \frac{1}{n.\hat{\lambda}_{st}}\sum_{i=1}^{n}\sum_{j \neq i} I_{(h,\Delta)}\,(d_{ij}, t_{ij}). \qquad (5)$$

167 Finally, we defined the space-time clustering (STC) measure, which reflects how much more likely it is that a
168 landslide will occur given a time and space distance from a previous landslide, as following:

169 Empirical $STC(h,\Delta) = \frac{\hat{K}(h,\Delta)}{K(h,\Delta)} - 1 \qquad (6)$

170 STC values > 0 indicate clustering and values < 0 indicate dispersion. We calculated STC (h, Δ) for a wide range

171 of h and Δ: values of h ranged from 0 to 500 meter in 30 steps, and values of Δ ranged from 0 to 38 years in 30

172 steps. This yielded 900 empirical values of STC (h, Δ). We then fitted an exponential decay function of h and Δ to

173 the empirical STC values. This exponential decay function was used to calculate STC values for each pixel

174 depending on when and where a landslide last occurred closely to that pixel.

175 Based on this, we calculated two landslide path dependency variables (Figure 5). The first variable reflects the

176 maximum value of all STC values for all previous landslides near a pixel. This variable results in high values when

177 one particular previous nearby landslide is expected to have a large impact on the susceptibility of landsliding. The

178 second variable is the sum of all STC values of all previous landslides near a pixel. This variable results in high

179 values when all previous nearby landslides are expected to have a large impact on the susceptibility of landsliding.

180 This approach mirrors what we did in our slope unit-based susceptibility model (Samia et al., 2018) in the sense

181 that the variables separate the impact of the most impactful previous nearby landslide from the impacts of all
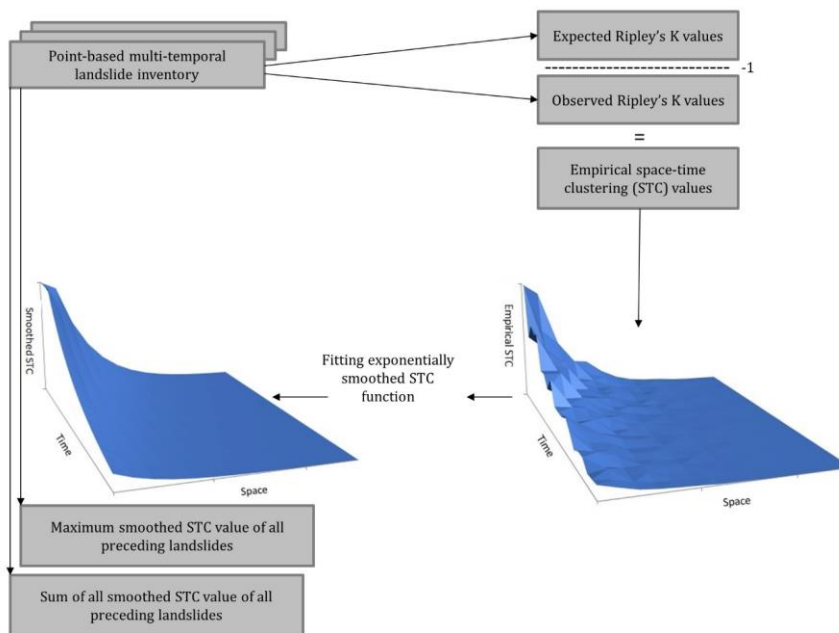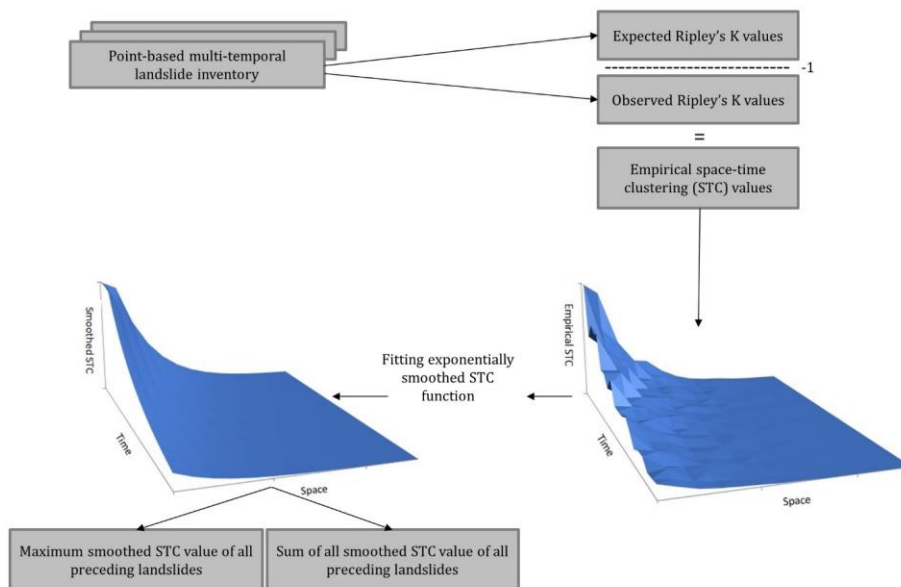
182 previous nearby landslides.

First diagram

Point-based multi-temporal landslide inventory →

- Expected Ripley's K values
- ------------------------------ -1
- Observed Ripley's K values
- =
- Empirical space-time clustering (STC) values

Empirical STC (Time / Space)

Fitting exponentially smoothed STC function

Smoothed STC (Time / Space)

- Maximum smoothed STC value of all preceding landslides
- Sum of all smoothed STC value of all preceding landslides

Second diagram

Point-based multi-temporal landslide inventory →

- Expected Ripley's K values
- ------------------------------ -1
- Observed Ripley's K values
- =
- Empirical space-time clustering (STC) values

Empirical STC (Time / Space)

Fitting exponentially smoothed STC function

Smoothed STC (Time / Space)

- Maximum smoothed STC value of all preceding landslides
- Sum of all smoothed STC value of all preceding landslides

183 **Figure 5.** Procedure to compute the two landslide path dependency variables using Ripley's space-time K function.

3.2 Logistic regression

185 Logistic regression is considered a reference model in statistically-based landslide susceptibility modelling
186 (Reichenbach et al., 2018). Relations between presence and absence of landslides as a binary target variable are
187 explained by a set of independent variables such as slope steepness and slope position in logistic regression. In
188 this paper, DEM-derivatives (section 2 and Figure 2) as well as the two landslide path dependency variables
189 computed using the Ripley's space-time K function (see section 3.1) were used as independent variables. Landslide
190 presence or absence was the binary target variable.

3.3 Training and testing

192 When using a multi-temporal landslide inventory in landslide susceptibility modelling, the selection of time slices
193 for the training and testing is crucial. In Rossi et al. (2010) and Samia et al. (2018), a sequential splitting sampling
194 strategy was used in such a way that landslides in older time slices were used to train the model and landslides in
195 newer time slices were used to test the model. However, such a sequential sampling strategy does not provide an
196 equal range of landslide histories between training and testing datasets and this could bias the role of time in path
197 dependent landslide susceptibility modelling. To avoid such a timing inequality, Samia et al. (2018) also
198 introduced a non-sequential sampling strategy in which the span of timing segregation among time slices in the
199 training and the testing datasets is comparable. In this study, we used this sampling strategy to split the multi-
200 temporal landslide inventory into training and testing datasets. To achieve this, all landslides in the time slices of
201 1947, 1954, 1981, 1985, 1999, May 2004, March and May 2010 were used for training, and all landslides in the
202 time slices of 1965, 1977, 1991, 1997, December 2004 and 2005 and April 2013 and 2014 were used for testing
203 (Figure 1). To achieve this, landslides in the time slices of 1947, 1954, 1981, 1985, 1999, May 2004, March and
204 May 2010 were used for training, and landslides in the time slices of 1965, 1977, 1991, 1997, December 2004 and
205 2005 and April 2013 and 2014 were used for testing (Figure 1). It is important to note that the time slice in 1939
206 was used only for quantification of landsliding history of the other time slices, and not for training or testing. Thus,
207 the 1st time slice in the training dataset is 1947 (Figure 1).

208 The number of pixels with landslides was smaller than the number of pixels without landslides in both training
209 and testing datasets. Therefore, we randomly selected 5,000 pixels with landslides and 5,000 pixels without
210 landslides from both training and testing datasets in order to create equal datasets both for training and testing of
211 the models. This random selection of pixels was repeated 10 times both in the training and testing datasets.
212 Therefore, we trained the conventional, conventional plus path dependent and purely path dependent landslide
213 susceptibility 10 times, and finally tested 10 times as well. After preparation of the 10 training datasets, logistic
214 regression was applied to the10 training datasets with entry probability of 0.05 and removal probability of 0.06 for
215 independent variables to diminish the chance of overfitting in the model. We only allowed inter-variable
216 correlations less than 0.8 to avoid multicollinearity. Conventional landslide susceptibility was modelled using
217 DEM-derivatives only once for the defined training dataset and was tested using the independent testing dataset.
218 Conventional plus path dependent landslide susceptibility model was constructed using DEM-derivatives plus the
219 two landslide path dependency variables. The purely path dependent landslide susceptibility was modelled only
220 by using the two landslide path dependency variables. All three models were constructed only once. Model

10

221 performance was assessed using AUC and AIC values. The AUC values for testing were assessed using 10 training
222 models and 10 independent testing datasets. The models with highest performance in terms of AUC values, were
223 used to map susceptibility to landslides. Finally, we compared landslide susceptibility maps resulting from
224 conventional, conventional plus path dependent and purely path dependent susceptibility.

4. Results

4.1 Spatial-temporal dynamic of landslide path dependency

227 Ripley's space-time K function confirmed the existence of landslide path dependency at small spatial and small
228 temporal distances from a previous landslide (Figure 6). The STC measure (Eq 6) is high in the space-time vicinity
229 of an earlier landslide, and it then decreases rapidly. Apparently, landslide susceptibility is relatively high
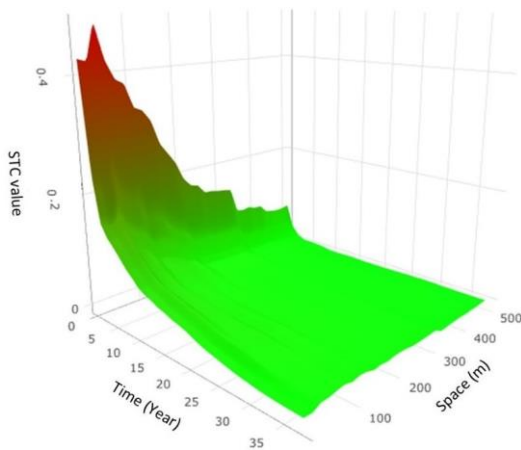230 immediately after occurrence of an earlier, nearby landslide.

231

232

233

Figure 6. Space-time dynamic of landslide path dependency. The colours represent the intensity of STC measure.
Red color indicates high STC and green indicates low STC.

236 The exponential decay function that was fitted to the empirical STC values is:

$$Smoothed\ STC(t,d) = 0.44 * e^{(-t/16.7)} * e^{(-d/58.8)} \qquad (7)$$

238 This function shows that the STC measure decays exponentially over a characteristic time scale of 16.7 years and
239 characteristic spatial scale of 58.8 meters. The residual standard error of the exponential function is 0.01, in units
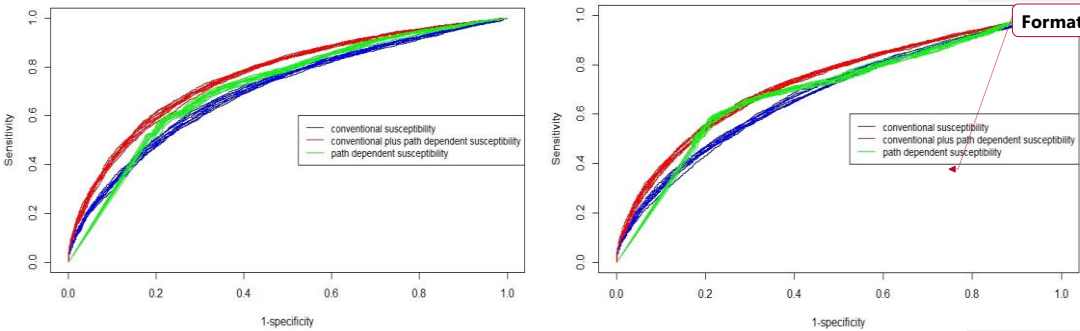240 of STC (-), which compares favourably with the actual values that range up to 0.44.

4.2 Model performance

11

We compared performance of the conventional, conventional plus path dependent, and purely path dependent landslide susceptibility models, using AUC (greater is better) and AIC (lower is better) values as measure of performance. The best performing landslide susceptibility model was the conventional plus path dependent model, both when expressed as AUC values and as AIC values (Table 1). The purely path dependent landslide susceptibility model, constructed with only the two landslide path dependency variables, performed better than the conventional landslide susceptibility model with its 16 DEM-derived variables.

Table 1. Performance of the three landslide susceptibility models. The values of AUC represent the average AUC values in the 10 training and 10 testing datasets. The values of AIC represent the average AIC values in the 10 training datasets.

AUC and AIC values	Conventional susceptibility model	Conventional plus path dependent susceptibility model	Path dependent susceptibility model
AUC training	0.704 ± 0.006	0.764 ± 0.003	0.721 ± 0.004
AIC training	$12{,}678 \pm 82$	$11{,}711 \pm 53$	$12{,}469 \pm 62$
AUC testing	0.682 ± 0.007	0.732 ± 0.004	0.698 ± 0.004

Figure 7. Receiver operating characteristic (ROC) curves of the three landslide susceptibility models in the 10 training datasets (left) and in the 10 testing datasets.

For conventional susceptibility models, 6 DEM-derivatives were selected in all 10 models (Table 2). Adding two landslide path dependency variables into DEM-derivatives variables affected the inclusion and exclusion of DEM-derivative variables only slightly. For example, the variables TPI and distance to river were selected 4 and 7 times respectively in the conventional susceptibility models whereas after adding the two landslide path dependency variables, these variables were selected 5 and 4 times respectively. The variable eastness which was selected twice in the conventional susceptibility models, was never selected in the conventional plus path dependent susceptibility models.

263 **Table 2.** Selection of independent variables in conventional, conventional plus path dependent and purely path
264 dependent landslide susceptibility modelling. Variables selected 6 or more times are shown. The numbers between
265 parentheses indicate how often variables were selected.

Three landslide susceptibility models	Number of variables selection in 10 times repetition	Average number of variables selected in the three susceptibility models
Conventional (16 DEM-derivatives)	Elevation (10), standard deviation of slope (10), LS factor (10), standard deviation of elevation (10), stream power index (10), aspect (10), distance to river (7), vertical distance to channel network (6), relative slope position (6)	8.7
Conventional plus path dependent (16 DEM-derivatives plus two landslide path dependency variables)	Elevation (10), standard deviation of slope (10), LS factor (10), standard deviation of elevation (10), stream power index (10), aspect (10), max smoothed STC value (10), sum of all smoothed STC value (10)	10.4
Path dependent (two landslide path dependency variables)	max smoothed STC value (10), sum of all smoothed STC value (10)	2

266

267 In all the training and the testing datasets, the contingency tables (Table 3) showed that conventional landslide
268 susceptibility models differed substantially from the conventional plus path dependent and path dependent
269 landslide susceptibility models. In particular, the percentage of false positives (the percentage of pixels without
270 landslides predicted with landslides) for the conventional susceptibility models is higher than for the two other
271 susceptibility models. However, there are also fewer true negatives (the percentage of pixels without landslides
272 predicted without landslides) in the conventional than in the conventional plus path dependent and path dependent
273 susceptibility models. The variation in the differences is larger in the training datasets than the testing datasets,
274 suggesting that all fitted models are robust.

275

276

277

278

279

280

281 **Table 3.** Contingency tables computed with cut off value of 0.5 for the three models. The numbers in the table
282 represent the average values computed in the 10 training and 10 testing datasets.

		Conventional landslide susceptibility		Conventional plus path dependent landslide susceptibility		Path dependent landslide susceptibility	
		Observed landslides		Observed landslides		Observed landslides	
		yes	no	yes	no	yes	no
Predicted landslides (training)	yes	35 ± 0.33	19 ± 0.60	34 ± 0.42	14 ± 0.23	31 ± 0.8	13 ± 0.32
	no	15 ± 0.33	31 ± 0.60	16 ± 0.42	36 ± 0.23	19 ± 0.8	37 ± 0.32
Predicted landslides (testing)	yes	33 ± 0.50	19 ± 0.21	29 ± 0.35	13 ± 0.43	23 ± 0.24	12 ± 0.41
	no	17 ± 0.50	31 ± 0.21	21 ± 0.35	37 ± 0.43	27 ± 0.24	38 ± 0.41

283

284 **3.3 Conventional, conventional plus path dependent and purely path dependent landslide susceptibility**
285 **maps**

286 The landslide susceptibility maps derived from the three models illustrate different patterns of landslide
287 susceptibility (Figure 78). For the models that include path dependency, the presented maps give the average values
288 of all simulated time slices. Differences between the maps correspond with the considerable differences in the
289 performance of their landslide susceptibility models in terms of AUC and AIC values (Table 1). The path
290 dependent landslide susceptibility map is visually different from both other landslide susceptibility maps, with the
291 pattern dominated by regions of high susceptibility around locations where landslides previously occurred.
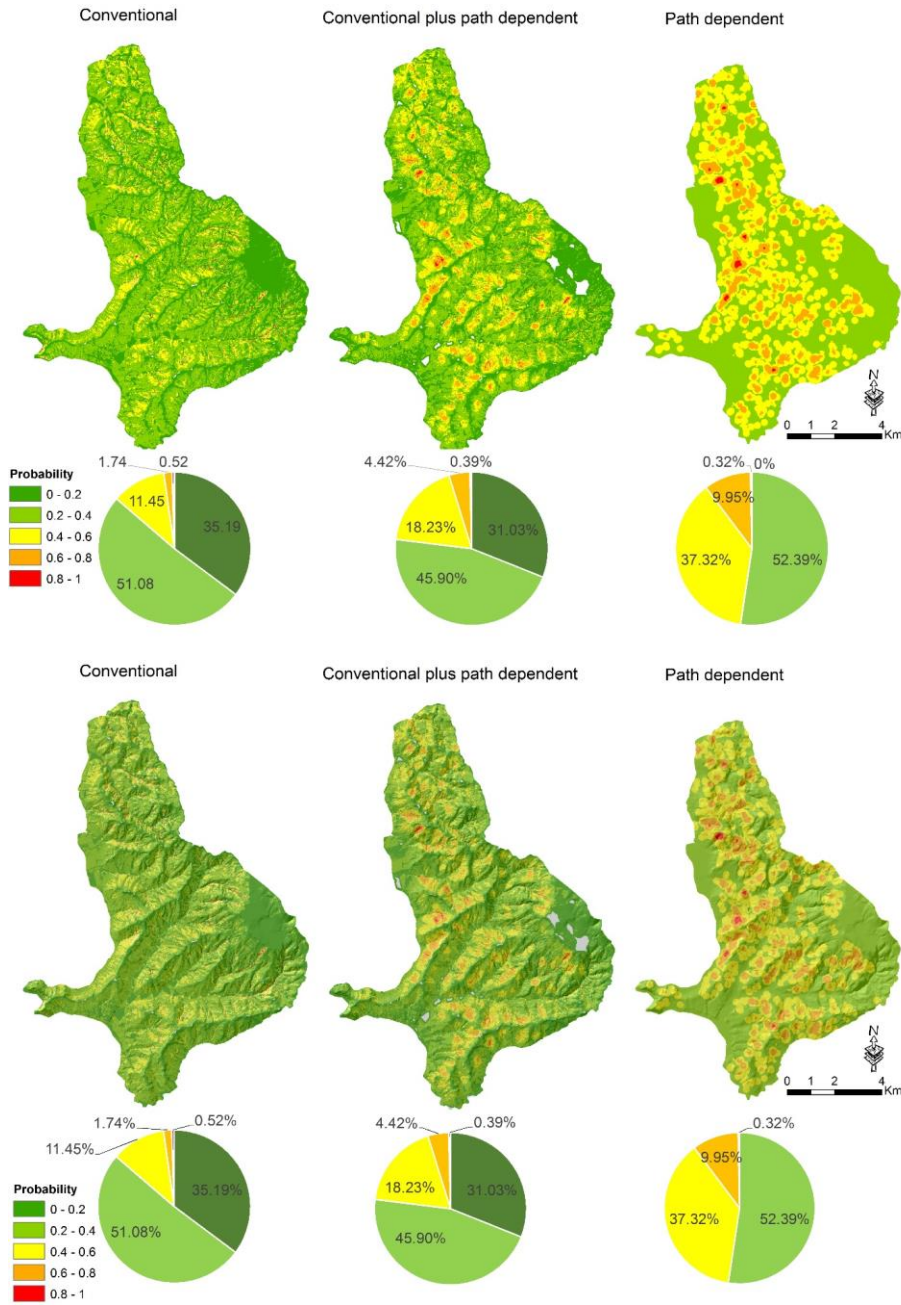
292

293

Figure 78. Conventional landslide susceptibility map in the left, the conventional plus path dependent landslide susceptibility map (averaged out over 16 time slices) in the middle and path dependent landslide susceptibility

15

296   map (averaged out over 16 time slices) in the right. The pie charts show the percentage of pixels in each map in

297   different probability levels of landslide occurrence.

298   The 16 conventional plus path dependent landslide susceptibility maps are dynamic and change over time (Figure

299   89). These changes reflect the exponential decay with increasing time since previous nearby landslides (Figure 6)

300   and the sudden increase of susceptibility in areas close to recent landslides. The gradual decrease in susceptibility

301   levels is clearest when comparing the 1981 and 2004 susceptibility maps, whereas the sudden increase is clearest

302   when comparing the 2004 and 2014 maps. The 2014 susceptibility map has higher susceptibility levels because of

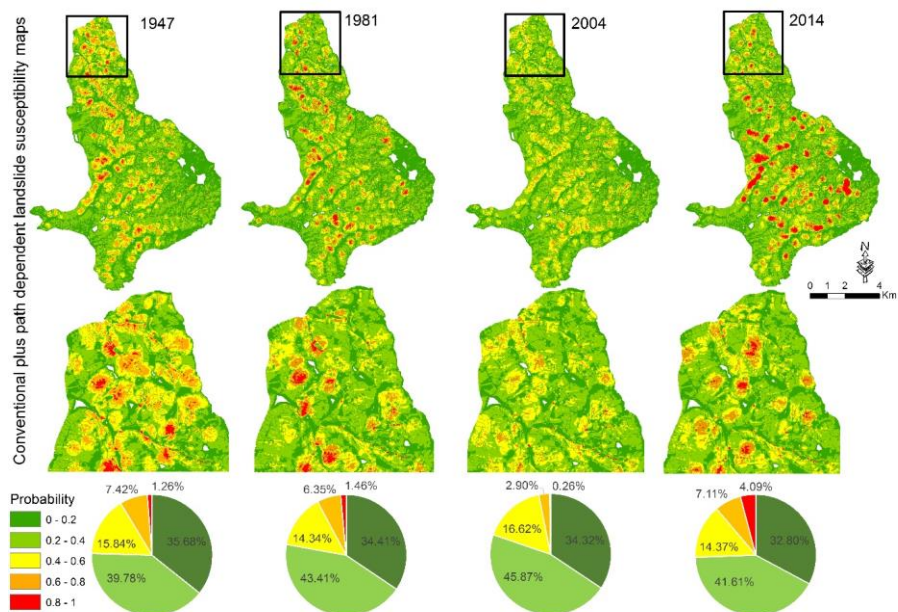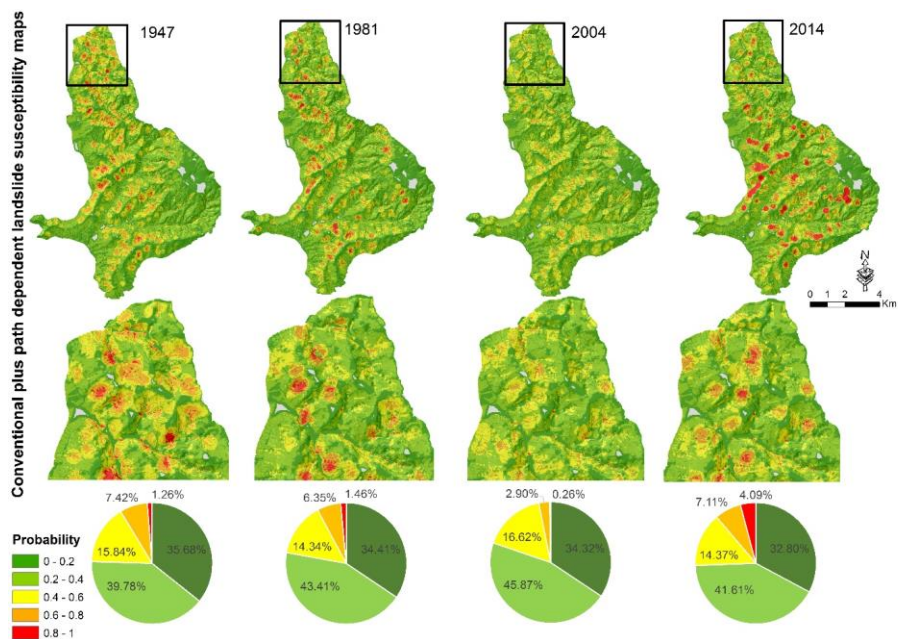303   the impact of recent landslides in the year 2013.

16

Conventional plus path dependent landslide susceptibility maps

Probability
- 0 - 0.2
- 0.2 - 0.4
- 0.4 - 0.6
- 0.6 - 0.8
- 0.8 - 1

305 **Figure 89.** Examples of four dynamic conventional plus path dependent landslide susceptibility maps in the years
306 of 1947, 1981, 2004 and 2014. Zoomed maps show the places where there are large changes in susceptibility over
307 time.

308 Similar dynamics are visible when comparing landslide susceptibility maps constructed with the purely path
309 dependent model for different years (Figure 910). These maps show only the pure influence of earlier landslides
310 on susceptibility to future landslides (Figure 6). Again, the susceptibility of landslides decreases where distance
311 from earlier landslides in space and time increases, but jumps back up when more recent landslides become part
312 of the landslide history. The pure influence of each individual landslide on the susceptibility to the future landslide
313 is strong when a landslide is fresh which is reflected in the high percentage of susceptibility levels of 0.6-0.8 and
314 0.8-1.0 in 1947 and 2014. When time passes since the previous landslide has occurred, the susceptibility decreases
315 with an exponential decay response which is reflected in the low percentage of susceptibility levels of 0.6-0.8 and
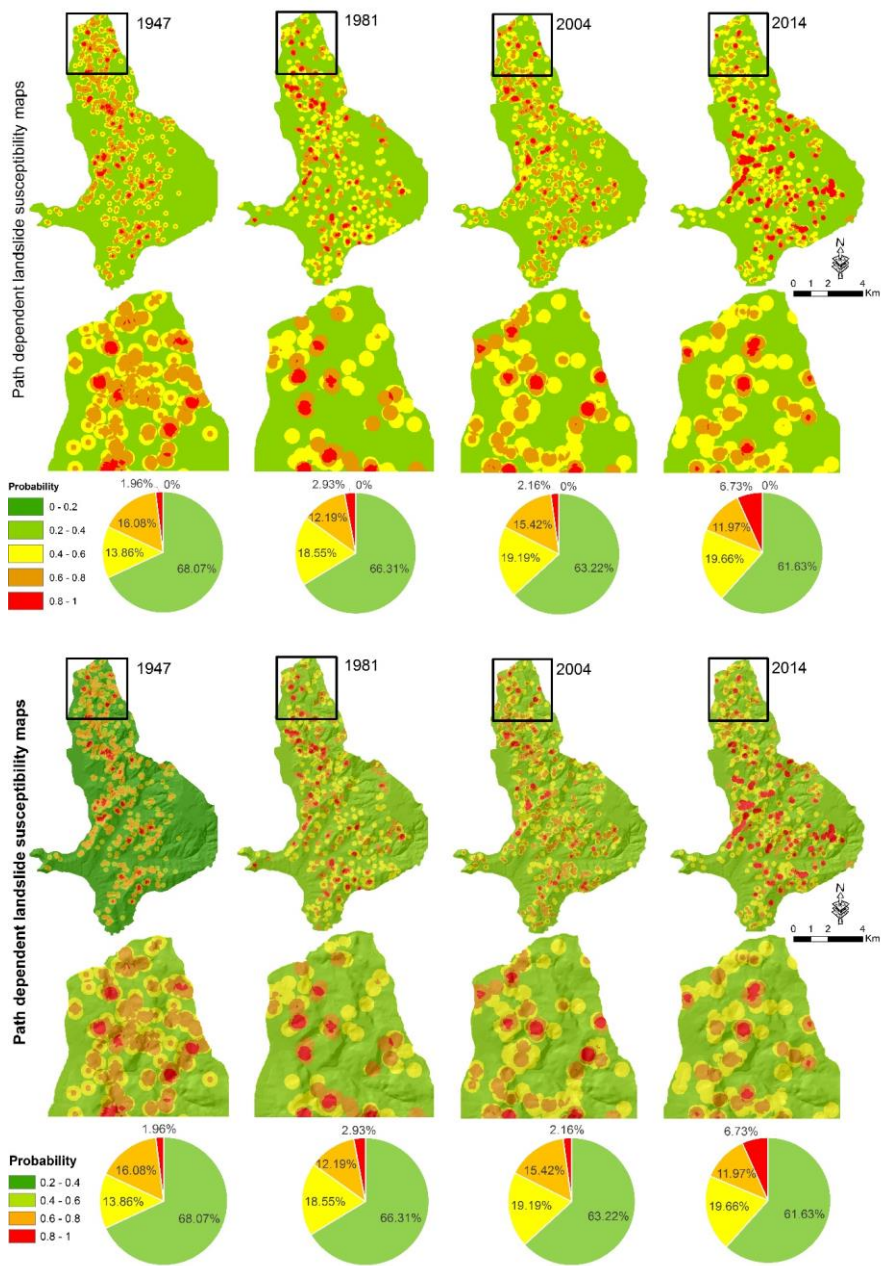316 0.8-1.0 in 1981 and 2004.

18

Figure 9̶10. Examples of four dynamic path dependent landslide susceptibility maps in the years of 1947, 1981, 2004 and 2014. Zoomed maps show the places where there are large changes in susceptibility over time.

19

5. Discussion

In this section, we focus first on the quantification of landslide path dependency in the pixel-based multi-temporal landslide inventory, and then discuss its role in susceptibility models. We also discuss the susceptibility model performance for all three model types. At the end, the exportability of landslide path dependency parameters and the implication of dynamic time-variant path dependent landslide susceptibility in landslide hazard is discussed.

5.1 Quantification of landslide path dependency

The quantification of landslide path dependency using Ripley's space-time K function (Ripley, 1976; Diggle et al., 1995) indicates, in our study area, an exponential decay response in the STC values (Figure 6). This means that there is a positive influence of earlier nearby landslides on susceptibility that decays exponentially in time and space with a characteristic time scale of about 17 years, and a characteristic space scale of about 60 meters. This is in accordance with our previously quantified landslide path dependency using follow-up landslide fraction in which the decay period of landslide path dependency was found to be about two decades (Samia et al., 2017b). Landslide clustering manifests in the form of spatial association among landslides where follow-up landslides occur immediately after and close to a previous landslide (Samia et al., 2017a). Samia et al. (2017b) discussed the possible mechanism in the formation of clusters of landslides in which the size of the initial landslide and changes in hydrology of slope destabilized by a landslide could facilitate the occurrence of follow-up landslides and hence clusters of landslides.

STC values and their exponential decay to some extent depend on the method that we have chosen to determine the centre point of landslides when converting polygons of landslides to points of landslides. Our approach was to take the geometric centre, but other options exist (Haines, 1994) and their impact should be explored. Also, in the computation of STC values with Ripley's space-time K function, distance between landslides was calculated using the Pythagorean theorem without distinguishing between distances in the x and y direction. Also we did not include differences in the elevation of centre points in our distance calculations. For future work, it could be interesting to define one dimension as the distance along the slope in the downslope direction and another dimension as the distance in the slope parallel direction, and keeping these two spatial dimensions separate in addition to the temporal dimension.

5.2 Effect of landslide path dependency on performance of landslide susceptibility models

Our results demonstrated that including landslide path dependency effect in a pixel-based landslide susceptibility model constructed by DEM-derivatives improves model performance substantially. This is in line with high AUC and low AIC values for the conventional plus path dependent landslide susceptibility model (Table 1 and Figure 7). This confirms our main hypothesis that adding the effect of landslide path dependency boosts the performance of landslide susceptibility models, and is in accordance with our previous expectations regarding stronger effect of landslide path dependency in a pixel-based landslide susceptibility model than in a slope unit-based landslide susceptibility model (Samia et al., 2018). Landslide path dependency is a local effect (apparently with characteristic space scale of about 60 meters) in which an earlier landslide increases the likelihood of follow-up landslide occurrence. Such a local effect is obviously more visible at pixel resolution of 10 m rather than at slope unit resolution (with a median size of 51486 m^2 in our study area).

20

Strikingly, the purely path dependent landslide susceptibility model constructed with only the two landslide path dependency variables performs better than the conventional landslide susceptibility model made by DEM-derivative variables (Table 1 and Figure 7). This is potentially interesting since it implies that the landslide inventory itself can be used to map susceptibility to landslide without using DEM-derivatives which have been conventionally used in landslide susceptibility modelling (Varnes, 1984; Guzzetti et al., 2005). More complex explanatory variables such as geology, soil and land use can also be used along with DEM-derivatives to improve landslide susceptibility models and maps. However, these are not always available. In fact, considering landslide path dependency effect into such complete explanatory factors improve their performance as well. We confirmed this in an additional exploration where we constructed a conventional landslide susceptibility model used in this paper, with the same DEM-derivatives, but also with land use and geology as explanatory factors. The results demonstrated that adding our two landslide path dependency variables to such an improved conventional landslide susceptibility increased its performance (from AUC value of 0.771 to AUC value of 0.801).

Another important aspect of considering landslide path dependency effect in landslide susceptibility modelling is providing dynamic landslide susceptibility maps. Landslide susceptibility maps are usually classified into five levels of probability to landslide occurrence ranging from 0 to 1. In the conventional landslide susceptibility map (Figure 78, right left map), the five probability levels of susceptibility by definition remain constant over time since the DEM-derivatives in the model are constant (although DEM-derivatives also change when a landslide occurs, but DEMs are not updated frequently enough to reflect this). The usage of conventional static landslide susceptibility maps and dynamic landslide susceptibility maps taking landslide path dependency depends on the goal and task of audience. In reality, static susceptibility maps created (either with a conventional susceptibility model, or as the static portion of a conventional plus path dependent model) with this time-insensitive method are can be used in sustainable planning whereas dynamic susceptibility maps can be considered in short-term land use planning. only for an amount of time roughly equal to the temporal length of the original landslide inventory.

However, adding landslide path dependency in landslide susceptibility models, provides dynamic landslide susceptibility maps (Figures 8 9 and 9 10) in which the levels of susceptibility change over time, reflecting the exponential decay response of landslide path dependency (Figure 6). The changes are in the places where landslides have already occurred, mainly in probability levels of susceptibility ranging from 0.6 to 1.0. This suggests that the part of area located in the high probability level of susceptibility could switch to the low probability level of susceptibility (0 to 0.6) after a decade. This is exemplified between 1947 and 1954 landslide susceptibility maps, in which about 9 km^2 of study area drops more than 0.1 in their probability of landslide occurrence. After adding the two path dependency variables in the conventional landslide susceptibility modelled with DEM-derivatives, it turns out that the coefficients of all DEM-derivative variables become lower (e.g., LS factor becomes less important).

5.3 Can landslide path dependency parameters be transported to other areas?

In landslide prone areas where landslides are documented and mapped in the form of polygon-based multi-temporal inventories, the landslide path dependency can be quantified based on geographical overlap among landslides, and hence used in landslide susceptibility modelling (Samia et al., 2017b; Samia et al., 2018). However,

394   polygon-based multi-temporal landslide inventories are rare to the best of our knowledge, and hence in many areas

395   geographical overlap among landslides cannot be computed. In this paper, we proposed using Ripley's space-time

396   K function to compute landslide path dependency where point-based multi-temporal landslide inventories are used.

397   Using such inventories, our STC measure (Eq. 6) can be used to quantify path dependency among landslides.

398   It is attractive to think that the STC measure (Eq. 6) and its parameters (Eq. 7) can be directly exported to landslide

399   prone areas with substantial geological and topographical similarities. However, to gain confidence in this

400   approach, multi-temporal landslide inventories from such places (e.g., (Schlögel et al., 2011)) need to be

401   interrogated to find out whether path dependency occurs, whether it occurs over similar space and time scales, and

402   whether it adds value to susceptibility modelling. This would also allow us to start exploring what determines the

403   characteristic space and time scales.

5.4 Implications of path dependent landslide susceptibility in landslide hazard assessment

405   We have already modified the definition of conventional landslide susceptibility modelling (Varnes, 1984;

406   Guzzetti et al., 2005) using spatial temporal dynamics of landslide path dependency (Samia et al., 2017a, b) as

407   following:

408    $Landslide\ susceptibility_{s,t} = f\big(conditioning\ attributes_s, landslide\ path\ dependency_{s,t}\big)$ (8)

409   In this study, both conventional plus path dependent and path dependent landslide susceptibility models turned out

410   to perform better than a conventional landslide susceptibility model (Table 1 and Figure 7). In both models,

411   availability of a space-time component – reflecting the exponential decay of landslide path dependency – indicates

412   that landslide susceptibility is dynamic. This challenges the way landslide hazard is assessed as landslide

413   susceptibility is an important element of landslide hazard.

414   In landslide hazard assessment, landslide susceptibility as a proxy of 'where landslides occur' is combined with

415   the temporal probability of landslide triggers (mainly rainfall) to determine 'when landslides occur' (Guzzetti et

416   al., 2006a). In this context, a dynamic landslide susceptibility (Eq. 8) needs to be considered in combination with

417   the temporal information of landslide triggers in the assessment of landslide hazard. When substantial landsliding

418   happens during a rainfall event, susceptibility in and around such landslides can be raised for a few decades in

419   which moderate rainfall events may already cause substantial landsliding, which raises susceptibility levels again.

420   (Figure 1011). If no substantial triggering event happens over the characteristic time scale of roughly 17 years, the

421   increased susceptibility will be substantially reduced, and a later rainfall event may have less influence on

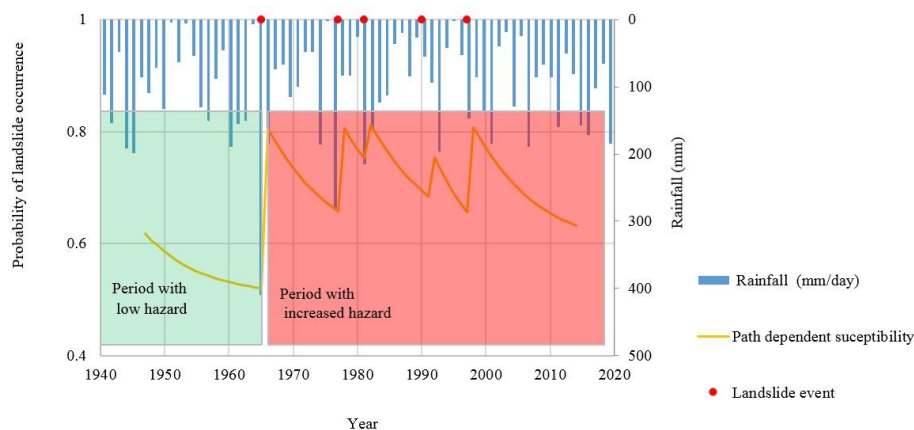422   landsliding; the probability of experiencing a follow-up landslide will have decreased.

Figure ~~10~~11. ~~Hypothetical example~~ <u>Conceptual model</u> of the implication of dynamic path dependent landslide susceptibility model in landslide hazard assessment. When susceptibility is low, the hazard is also low (providing the other components of landslide hazard e.g., size remain unchanged) and large rainfall events are needed to trigger new landslides. Then, when susceptibility is raised by such landslides, the hazard is also high and small rainfall events may trigger new landslides.

6. **Conclusion**

In the Collazzone study area, in Central Italy, quantification of landslide path dependency reveals an exponential decay response in landslide susceptibility as a function of space and time distance to earlier nearby landslides. For our study area, the characteristic time scale of this effect is about 17 years and the characteristic space scale is about 60 meters. Adding such an exponential decay response of landslide path dependency in conventional pixel-based landslide susceptibility modelled by DEM-derivative improves the performance of model substantially. Taking into account landslide path dependency effects in landslide susceptibility results in dynamic landslide susceptibility models where susceptibility changes over time. We stress that landslide susceptibility modelling should take the effect of landslide path dependency into account since it provides an estimation of temporal validation of different probability levels of landslide occurrence in landslide susceptibility map. The obtained landslide path dependency parameters can possibly be used for dynamic landslide susceptibility modelling in landslide prone areas with environmental and data similarities. We proposed a conceptual model that considers the impact of dynamic path dependent landslide susceptibility on landslide hazard.

References

447 **References**

448 Akaike, H.: Information theory and an extension of the maximum likelihood principle, in: Selected Papers of
449 Hirotugu Akaike, Springer, 199-213, 1998.
450 Alvioli, M., Marchesini, I., Reichenbach, P., Rossi, M., Ardizzone, F., Fiorucci, F., and Guzzetti, F.: Automatic
451 delineation of geomorphological slope units with r.slopeunits v1.0 and their optimization for landslide
452 susceptibility modeling, Geosci. Model Dev., 9, 3975-3991, 10.5194/gmd-9-3975-2016, 2016.
453 Ardizzone, F., Cardinali, M., Galli, M., Guzzetti, F., and Reichenbach, P.: Identification and mapping of recent
454 rainfall-induced landslides using elevation data collected by airborne Lidar, Natural Hazards and Earth System
455 Science, 7, 637-650, 2007.
456 Ardizzone, F., Fiorucci, F., Santangelo, M., Cardinali, M., Mondini, A. C., Rossi, M., Reichenbach, P., and
457 Guzzetti, F.: Very-high resolution stereoscopic satellite images for landslide mapping, in: Landslide science and
458 practice, Springer, 95-101, 2013.
459 Ardizzone, F., Fiorucci, F., Mondini, A. C., and Guzzetti, F.: TXT-tool 1.039-1.1: Very-High Resolution Stereo
460 Satellite Images for Landslide Mapping, in: Landslide Dynamics: ISDR-ICL Landslide Interactive Teaching Tools
461 : Volume 1: Fundamentals, Mapping and Monitoring, edited by: Sassa, K., Guzzetti, F., Yamagishi, H., Arbanas,
462 Ž., Casagli, N., McSaveney, M., and Dang, K., Springer International Publishing, Cham, 83-94, 2018.
463 Brabb, E. E.: Innovative approaches to landslide hazard and risk mapping, International Landslide Symposium
464 Proceedings, Toronto, Canada, 1985, 17-22,
465 Cardinali, M., Ardizzone, F., Galli, M., Guzzetti, F., and Reichenbach, P.: Landslides triggered by rapid snow
466 melting: the December 1996–January 1997 event in Central Italy, Proceedings 1st Plinius Conference on
467 Mediterranean Storms, 2000, 439-448,
468 Carrara, A., Cardinali, M., Detti, R., Guzzetti, F., Pasqui, V., and Reichenbach, P.: GIS techniques and statistical
469 models in evaluating landslide hazard, Earth surface processes and landforms, 16, 427-445, 1991.
470 Costanzo, D., Rotigliano, E., Irigaray Fernández, C., Jiménez-Perálvarez, J. D., and Chacón Montero, J.: Factors
471 selection in landslide susceptibility modelling on large scale following the gis matrix method: application to the
472 river Beiro basin (Spain), 2012.
473 Diggle, P. J., Chetwynd, A. G., Häggkvist, R., and Morris, S. E.: Second-order analysis of space-time clustering,
474 Statistical methods in medical research, 4, 124-136, 1995.
475 Galli, M., Ardizzone, F., Cardinali, M., Guzzetti, F., and Reichenbach, P.: Comparing landslide inventory maps,
476 Geomorphology, 94, 268-289, 2008.
477 Gavin, D. G., Hu, F. S., Lertzman, K., and Corbett, P.: WEAK CLIMATIC CONTROL OF STAND-SCALE FIRE
478 HISTORY DURING THE LATE HOLOCENE, Ecology, 87, 1722-1732, 2006.
479 Gorum, T., Fan, X., van Westen, C. J., Huang, R. Q., Xu, Q., Tang, C., and Wang, G.: Distribution pattern of
480 earthquake-induced landslides triggered by the 12 May 2008 Wenchuan earthquake, Geomorphology, 133,
481 152-167, https://doi.org/10.1016/j.geomorph.2010.12.030, 2011.
482 Günther, A., Van Den Eeckhaut, M., Malet, J.-P., Reichenbach, P., and Hervás, J.: Climate-physiographically
483 differentiated Pan-European landslide susceptibility assessment using spatial multi-criteria evaluation and
484 transnational landslide information, Geomorphology, 224, 69-85,
485 https://doi.org/10.1016/j.geomorph.2014.07.011, 2014.
486 Guzzetti, F., Reichenbach, P., Cardinali, M., Galli, M., and Ardizzone, F.: Probabilistic landslide hazard
487 assessment at the basin scale, Geomorphology, 72, 272-299, 2005.
488 Guzzetti, F., Galli, M., Reichenbach, P., Ardizzone, F., and Cardinali, M.: Landslide hazard assessment in the
489 Collazzone area, Umbria, Central Italy, Natural Hazards and Earth System Science, 6, 115-131, 2006a.
490 Guzzetti, F., Reichenbach, P., Ardizzone, F., Cardinali, M., and Galli, M.: Estimating the quality of landslide
491 susceptibility models, Geomorphology, 81, 166-184, https://doi.org/10.1016/j.geomorph.2006.04.007, 2006b.
492 Guzzetti, F., Ardizzone, F., Cardinali, M., Rossi, M., and Valigi, D.: Landslide volumes and landslide mobilization
493 rates in Umbria, central Italy, Earth and Planetary Science Letters, 279, 222-229,
494 https://doi.org/10.1016/j.epsl.2009.01.005, 2009.
495 Guzzetti, F., Mondini, A. C., Cardinali, M., Fiorucci, F., Santangelo, M., and Chang, K.-T.: Landslide inventory
496 maps: New tools for an old problem, Earth-Science Reviews, 112, 42-66, 2012.
497 Haines, E.: Point in polygon strategies, Graphics gems IV, 994, 24-26, 1994.
498 Hinman, S. E., Blackburn, J. K., and Curtis, A.: Spatial and temporal structure of typhoid outbreaks in
499 Washington, DC, 1906–1909: evaluating local clustering with the G i* statistic, International Journal of Health
500 Geographics, 5, 13, 2006.
501 Jebur, M. N., Pradhan, B., and Tehrany, M. S.: Optimization of landslide conditioning factors using very high-
502 resolution airborne laser scanning (LiDAR) data at catchment scale, Remote Sensing of Environment, 152, 150-
503 165, 2014.
504 Keefer, D. K.: Statistical analysis of an earthquake-induced landslide distribution — the 1989 Loma Prieta,
505 California event, Engineering Geology, 58, 231-249, https://doi.org/10.1016/S0013-7952(00)00037-5, 2000.
506 Levine, N.: Crime mapping and the Crimestat program, Geographical analysis, 38, 41-56, 2006.
507 Lynch, H. J., and Moorcroft, P. R.: A spatiotemporal Ripley's K-function to analyze interactions between spruce
508 budworm and fire in British Columbia, Canada, Canadian Journal of Forest Research, 38, 3112-3119, 2008.
509 Mason, S. J., and Graham, N. E.: Areas beneath the relative operating characteristics (ROC) and relative
510 operating levels (ROL) curves: Statistical significance and interpretation, Quarterly Journal of the Royal
511 Meteorological Society, 128, 2145-2166, 2002.
512 Moore, I. D., and Wilson, J. P.: Length-slope factors for the Revised Universal Soil Loss Equation: Simplified
513 method of estimation, Journal of soil and water conservation, 47, 423-428, 1992.
514 Moore, I. D., Gessler, P., Nielsen, G., and Peterson, G.: Soil attribute prediction using terrain analysis, Soil
515 Science Society of America Journal, 57, 443-452, 1993.

516 Neuhäuser, B., Damm, B., and Terhorst, B.: GIS-based assessment of landslide susceptibility on the base of the
517 weights-of-evidence model, Landslides, 9, 511-528, 2012.
518 Phillips, J.: Evolutionary geomorphology: thresholds and nonlinearity in landform response to environmental
519 change, 2006.
520 Reichenbach, P., Rossi, M., Malamud, B. D., Mihir, M., and Guzzetti, F.: A review of statistically-based landslide
521 susceptibility models, Earth-Science Reviews, 180, 60-91, https://doi.org/10.1016/j.earscirev.2018.03.001,
522 2018.
523 Riley, S. J., DeGloria, S., and Elliot, R.: Index that quantifies topographic heterogeneity, intermountain Journal
524 of sciences, 5, 23-27, 1999.
525 Ripley, B. D.: The second-order analysis of stationary point processes, Journal of applied probability, 13, 255-
526 266, 1976.
527 Ripley, B. D.: Modelling spatial patterns, Journal of the Royal Statistical Society. Series B (Methodological),
528 172-212, 1977.
529 Rossi, M., Guzzetti, F., Reichenbach, P., Mondini, A. C., and Peruccacci, S.: Optimal landslide susceptibility
530 zonation based on multiple forecasts, Geomorphology, 114, 129-142,
531 https://doi.org/10.1016/j.geomorph.2009.06.020, 2010.
532 Samia, J., Temme, A., Bregt, A., Wallinga, J., Guzzetti, F., Ardizzone, F., and Rossi, M.: Do landslides follow
533 landslides? Insights in path dependency from a multi-temporal landslide inventory, Landslides, 14, 547-558,
534 10.1007/s10346-016-0739-x, 2017a.
535 Samia, J., Temme, A., Bregt, A., Wallinga, J., Guzzetti, F., Ardizzone, F., and Rossi, M.: Characterization and
536 quantification of path dependency in landslide susceptibility, Geomorphology, 292, 16-24,
537 https://doi.org/10.1016/j.geomorph.2017.04.039, 2017b.
538 Samia, J., Temme, A., Bregt, A. K., Wallinga, J., Stuiver, J., Guzzetti, F., Ardizzone, F., and Rossi, M.:
539 Implementing landslide path dependency in landslide susceptibility modelling, Landslides, 1-16, 2018.
540 Sato, H. P., Hasegawa, H., Fujiwara, S., Tobita, M., Koarai, M., Une, H., and Iwahashi, J.: Interpretation of
541 landslide distribution triggered by the 2005 Northern Pakistan earthquake using SPOT 5 imagery, Landslides, 4,
542 113-122, 10.1007/s10346-006-0069-5, 2007.
543 Schlögel, R., Torgoev, I., De Marneffe, C., and Havenith, H. B.: Evidence of a changing size−frequency
544 distribution of landslides in the Kyrgyz Tien Shan, Central Asia, Earth Surface Processes and Landforms, 36,
545 1658-1669, 2011.
546 Smith, T.: Notebook on spatial data analysis, Lecture Note, 2016.
547 Tonini, M., Pedrazzini, A., Penna, I., and Jaboyedoff, M.: Spatial pattern of landslides in Swiss Rhone Valley,
548 Natural Hazards, 73, 97-110, 2014.
549 Van Westen, C., Rengers, N., and Soeters, R.: Use of geomorphological information in indirect landslide
550 susceptibility assessment, Natural hazards, 30, 399-419, 2003.
551 Van Westen, C. J., Castellanos, E., and Kuriakose, S. L.: Spatial data for landslide susceptibility, hazard, and
552 vulnerability assessment: an overview, Engineering geology, 102, 112-131, 2008.
553 Varnes, D. J.: Landslide hazard zonation: a review of principles and practice, 1984.
554 Ye, X., Xu, X., Lee, J., Zhu, X., and Wu, L.: Space−time interaction of residential burglaries in Wuhan, China,
555 Applied Geography, 60, 210-216, https://doi.org/10.1016/j.apgeog.2014.11.022, 2015.

556